Langmuir
Article
pubs.acs.org/Langmuir

Mapping the Local Osmotic Modulus of Polymer Gels†

Ferenc Horkay* and David C. Lin

Section on Tissue Biophysics and Biomimetics, Program in Physical Biology, Eunice Kennedy Shriver National Institute of Child Health and Human Development, National Institutes of Health, Bethesda, Maryland 20892

Received January 9, 2009. Revised Manuscript Received February 17, 2009

Polymer gels undergo volume phase transition in a thermodynamically poor solvent as a result of changes in molecular interactions. The osmotic pressure of gels, both synthetic and biological in nature, induces swelling and imparts the materials with the capacity to resist compressive loads. We have investigated the mechanical and swelling properties of poly(vinyl alcohol) (PVA) gels brought into the unstable state by changing the composition of the solvent. Chemically cross-linked PVA gels were prepared and initially swollen in water at 25 °C, and then *n*-propyl alcohol (nonsolvent) was gradually added to the equilibrium liquid. AFM imaging and force−indentation measurements were made in water/*n*-propyl alcohol mixtures of different composition. It has been found that the elastic modulus of the gels exhibits simple scaling behavior as a function of the polymer concentration in each solvent mixture over the entire concentration range investigated. The power law exponent *n* obtained for the concentration dependence of the shear modulus increases from 2.3 (in pure water) to 7.4 (in 35% (v/v) water + 65% (v/v) *n*-propyl alcohol mixture). In the vicinity of the Θ-solvent composition (59% (v/v) water + 41% (v/v) *n*-propyl alcohol) $n \approx 2.9$. Shear and osmotic modulus maps of the phase separating gels have been constructed. It is demonstrated that the latter sensitively reflects the changes both in the topography and thermodynamic interactions occurring in the course of volume phase transition.

1. Introduction

A polymer network is a macroscopic assembly of long polymer molecules joined at several connection sites (cross-links). The cross-links can be either chemical or physical bonds. Gels may involve different types of interactions, such as hydrogen bonds, electrostatic interactions (e.g., ion bridges), hydrophobic interactions, etc. In gels the cross-link distribution is always inhomogeneous. Upon swelling, the weakly cross-linked regions swell more, while the densely cross-linked regions swell less. The difference in swelling causes nonuniformity of the local elastic properties.

As an innate property of gels and soft tissues, the elastic modulus is often associated with the equilibrium mechanical response of the system. At the bulk material level, this quantity serves as a measure of small deformation behavior and can be used, for example, to compare the compressive stiffness of tissues at different stages of development.[1,2] Articular cartilage exemplifies the compositional and structural complexities found in soft tissues.[3−6] The elastic modulus is also intrinsic to various mathematical models, both phenomenological and molecular in nature, that describe the load−deformation behavior of these materials. While the relationship between composition and material behavior is consequential at the bulk level, it becomes nontrivial at smaller length scales, where local variations in mechanical properties are affected by changes in the structure and interactions among the constituents. Even the most sophisticated constitutive models, however, consider composition only implicitly.

Despite significant differences in composition, synthetic and biological gels exhibit qualitatively similar responses (e.g., viscoelasticity and nonlinear stress−strain behavior at large deformation) under various loading conditions since they are governed by common physical principles.[7] Biological tissues are always inhomogeneous; i.e., their local mechanical and osmotic properties strongly differ from those at the macroscopic level.

The atomic force microscope (AFM) is a powerful device to map the elastic and structural features of synthetic and biological gels at nanometer resolution.[8−11] The force sensitivity of AFM cantilevers allows us to detect heterogeneities in gels that appear uniform at lower resolutions[9,12−19] as well as to reveal the correspondence between mechanical and structural features in soft tissues (e.g., cells and their extracellular matrix can be delineated by their dissimilarity in stiffness[20,21]). However, previous AFM studies have shown that the shear modulus only weakly varies even in highly inhomogeneous biological tissues such as the extracellular matrix of mouse cartilage.[21] This finding

† Part of the Gels and Fibrillar Networks: Molecular and Polymer Gels and Materials with Self-Assembled Fibrillar Networks special issue.

*Corresponding author. E-mail: horkay@helix.nih.gov.

(1) Kempson, G. E. *Biochim. Biophys. Acta* **1991**, *1075*, 223–230.
(2) Williamson, A. K.; Chen, A. C.; Masuda, K.; Thonar, E. J.; Sah, R. L. *J. Orthop. Res.* **2003**, *21*, 872–880.
(3) Kovach, I. S. *Biophys. Chem.* **1995**, *53*, 181–187.
(4) Mow, V. C.; Guo, X. E. *Annu. Rev. Biomed. Eng.* **2002**, *4*, 175–209.
(5) Narmoneva, D. A.; Wang, J. Y.; Setton, L. A. *Biophys. J.* **2001**, *81*, 3066–3076.
(6) Urban, J. P.; Maroudas, A.; Bayliss, M. T.; Dillon, J. *Biorheology* **1979**, *16*, 447–464.
(7) Holzapfel, G. A. In *Constitutive Models for Rubber IV*; Austrell, P. E., Keri, L., Eds.; A. A. Balkema Publishers: Leiden, 2005; pp 607−617.
(8) Ludwig, T.; Kirmse, R.; Poole, K.; Schwarz, U. S. *Pflugers Arch.* **2008**, *456*, 29–49.
(9) Opdahl, A.; Hoffer, S.; Mailhot, B.; Somorjai, G. A. *Chem. Rec.* **2001**, *1*, 101–122.
(10) Vinckier, A.; Semenza, G. *FEBS Lett.* **1998**, *430*, 12–16.
(11) You, H. X.; Yu, L. *Methods Cell Sci.* **1999**, *21*, 1–17.
(12) Domke, J.; Radmacher, M. *Langmuir* **1998**, *14*, 3320–3325.
(13) Eaton, P.; Smith, J. R.; Graham, P.; Smart, J. D.; Nevell, T. G.; Tsibouklis, J. *Langmuir* **2002**, *18*, 3387–3389.
(14) Lin, D. C.; Dimitriadis, E. K.; Horkay, F. *eXPRESS Polym. Lett.* **2007**, *1*, 576–584.
(15) Nie, H. Y.; Motomatsu, M.; Mizutani, W.; Tokumoto, H. *Thin Solid Films* **1996**, *273*, 143–148.
(16) Nitta, T.; Haga, H.; Kawabata, K.; Abe, K.; Sambongi, T. *Ultramicroscopy* **2000**, *82*, 223–226.
(17) Radmacher, M.; Fritz, M.; Hansma, P. K. *Biophys. J.* **1995**, *69*, 264–270.
(18) Tsukruk, V. V.; Huang, Z. *Polymer* **2000**, *41*, 5541–5545.
(19) VanLandingham, M. R.; Villarrubia, J. S.; Guthrie, W. F.; Meyers, G. F. *Macromol. Symp.* **2001**, *167*, 15–43.
(20) Allen, D. M.; Mao, J. J. *J. Struct. Biol.* **2004**, *145*, 196–204.
(21) Lin, D. C.; Shreiber, D. I.; Dimitriadis, E. K.; Horkay, F., *Biomech. Model. Mechanobiol.*, in press.

implies that the elastic modulus is not particularly sensitive to changes in the interactions between either the polymer and the solvent or the polymer molecules themselves.

In general, the swelling pressure of a gel is determined by the difference between the osmotic pressure of the cross-linked polymer and the elastic pressure of the swollen network.[22] Changes in the thermodynamic quality of the solvent strongly affect the osmotic contribution of the swelling pressure while the elastic term is only slightly influenced.[23,24] Thus, a sensitive indicator of changes in the thermodynamic properties should explicitly contain the contribution from the osmotic pressure.

In polymer physics, the osmotic modulus K is used to quantify the volume resistance of gels to an applied compressive load that encompasses not only the elastic properties of the material but also its composition and interactions with its environment.[24] Construction of maps of the osmotic and elastic moduli that reflect the effect of spatial variations of concentration fluctuations on these quantities has great potential in understanding the balance between the osmotic and elastic forces in complex biological samples, such as tissues and cells that are intrinsically inhomogeneous. For example, the load-bearing capacity of cartilage is governed by the osmotic modulus of the highly charged aggrecan/hyaluronic complexes enmeshed in the collagen matrix.[3−6,25] The collagen fibrils (collagen molecules packed into overlapping organized bundles) are arranged in different combinations and concentrations in various tissues to provide the required biomechanical properties. Knowledge of the local structure and physical properties of the collagen matrix as well as the mechanism of fiber formation is particularly important to better understanding how tissues are constructed in growth and repair and change in development and disease.

In this paper we introduce a method to create osmotic modulus maps by combining swelling pressure measurements and high-resolution AFM force−indentation measurements. To illustrate the feasibility of this procedure, we investigate the macroscopic and microscopic elastic and osmotic moduli of a model polymer gel in which phase separation is induced by gradually varying the thermodynamic quality of the solvent. The gel system studied in this work is cross-linked poly(vinyl alcohol) (PVA) swollen in water/*n*-propyl alcohol mixtures of various *n*-propyl alcohol contents [from 0 to 65% (v/v)]. Water is a relatively good solvent for the PVA chains while *n*-propyl alcohol is a nonsolvent. In solvent/nonsolvent mixtures containing more than ∼45% (v/v) *n*-propyl alcohol PVA gels become turbid and shrink. It will be shown that the osmotic modulus map reveals fine scale variations in the osmotic response due to changes in the molecular interactions among the components.

The paper is structured as follows: After a brief description of the theory of gel swelling we present experimental results obtained by macroscopic measurements with particular emphasis on the effect of solvent quality on the concentration dependence of the elastic (shear) modulus. A scaling formalism is employed to analyze the data. Imaging results and elasticity measurements made by the AFM are then discussed. The procedure proposed to determine the osmotic modulus maps from AFM force−indentation measurements in conjunction with macroscopic swelling pressure observations is described. Illustrative examples of osmotic and shear modulus maps are presented for lightly cross-linked PVA gels swollen in water/*n*-propyl alcohol mixtures of different composition.

2. Theoretical Section

2.1. General Considerations. Since the pioneering works of Dusek[26,27] and Tanaka[24,28] it is known that polymer gels may undergo a volume transition as experimental conditions, such as temperature, pressure, solvent composition, ionic strength, and pH, vary. Flory,[22] James and Guth,[29,30] Hermans,[31] and others proposed various statistical mechanical models to estimate the free energy change accompanied by the deformation and swelling of polymer networks. Experimental studies made on weakly cross-linked neutral gels [e.g., poly(*N*-isopropylacrylamide) gels (PNIPAM)] as well as polyelectrolyte gels indicated a rather sharp volume change as a function of the temperature or ionic strength.[32] These observations have been interpreted as a discontinuous volume transition. Continuous volume changes have also been reported for gels. For example, Li and Tanaka[33] found that the discontinuous volume transition of PNIPAM hydrogels becomes continuous as the cross-link density increases.

On the microscopic level the polymer gel is composed of closely packed polymer coils kept together by the cross-links. Gel swelling (or shrinking) is related to the expansion (or contraction) of the network chains. In general, the radius of gyration of the individual chains consisting of N monomeric units is given as

$$R \propto N^{\nu} \tag{1}$$

where ν is a universal exponent, the value of which is governed by the effective interaction between the polymer segments and the solvent molecules.[34] In good solvent condition ($\nu \approx 3/5$) the monomer−monomer interaction is repulsive and tends to swell the chain (strong excluded volume interaction). In a Θ-solvent where the attractive and repulsive forces compensate, the polymer exhibits ideal behavior (no excluded volume interaction), i.e., $\nu = 1/2$. In a poor solvent the attractive interactions between polymer segments dominate, the chains collapse, and $\nu = 1/3$. In polymer solutions, the decrease in solvent quality leads to phase separation, and beyond the critical point a solvent-rich phase will coexist with a polymer-rich phase.

In gels, however, permanent cross-links prohibit the network chains from changing relative positions. As the solvent quality decreases, the concentration fluctuations increase and the gel starts to shrink. The elastic stress due to chain deformation is coupled to the local concentration fluctuations. Polymer-rich domains are formed as a result of the segregation process. The size and shape of these domains depend on the particular polymer−solvent system, the cross-link density, and the actual geometry of the gel sample.

2.2. Elastic and Swelling Properties of Polymer Networks. Simple scaling theory[34] derives the behavior of neutral polymer gels from the properties of the corresponding solutions at the overlap concentration φ^*. At φ^* the average polymer

(22) Flory, P. J. *Principles of Polymer Chemistry*; Cornell University Press: Ithaca, NY, 1953.
(23) Zrinyi, M.; Horkay, F. *J. Polym. Sci., Part B* **1982**, *20*, 815–823.
(24) Tanaka, T.; Fillmore, D. J. *J. Chem. Phys.* **1979**, *70*, 1214–1218.
(25) Maroudas, A. I. *Nature (London)* **1976**, *260*, 808–809.
(26) Dusek, K.; Patterson, D. *J. Polym. Sci., Part A-2* **1968**, *6*, 1209–1216.
(27) Dusek, K.; Prins, W. *Adv. Polym. Sci.* **1969**, *6*, 1–102.
(28) Tanaka, T.; Swislow, G. *Phys. Rev. Lett.* **1979**, *42*, 1556–1559.
(29) James, H. M.; Guth, E. *J. Chem. Phys.* **1943**, *11*, 455–481.
(30) James, H. M.; Guth, E. *J. Chem. Phys.* **1947**, *15*, 669–683.
(31) Hermans, J. J. *J. Polym. Sci.* **1962**, *59*, 191–208.
(32) Wu, C.; Zhou, S. *J. Polym. Sci., Part B* **1996**, *34*, 1597–1604.
(33) Li, Y.; Tanaka, T. *J. Chem. Phys.* **1989**, *90*, 5161–5166.
(34) De Gennes, P. G. *Scaling Concepts in Polymer Physics*; Cornell University Press: Ithaca, NY, 1979.

concentration of the system is equal to that of an individual swollen coil.

The concentration of the fully swollen gel φ_e is proportional to φ^*. The latter can be expressed as[34]

$$\varphi_e \propto \varphi^* \propto N/R^3 \propto N^{1-3\nu} \quad (2)$$

In neutral gels interactions between the polymer chains are not expected to contribute significantly to the elastic properties; i.e., the elastic modulus is primarily governed by the concentration of the network chains. The shear modulus of a fully swollen gel G_e is given by

$$G_e = Ak_BT\frac{\varphi_e}{N} \quad (3)$$

where A is a constant, k_B is the Boltzmann factor, and T is the absolute temperature. Since φ_e and N are related by eq 2, for gels differing in the cross-link density the concentration dependence of G_e should obey the scaling relation

$$G_e = Ak_BT{\varphi_e}^{3\nu/(3\nu-1)} \quad (4)$$

Equation 4 predicts that the power law exponent n is $\approx 9/4$ in good solvent and 3 in Θ-solvent conditions. In the poor solvent regime n increases and diverges in the $\nu \rightarrow 1/3$ limit. However, in poor solvent condition, the validity of simple scaling relationships becomes questionable because of the high polymer concentration of the gel.

The elastic modulus defines the elastic pressure ($\Pi_{el} = -G$) that contracts the gel while the osmotic pressure expands it. At equilibrium in excess amount of solvent the elastic pressure balances the osmotic pressure Π_{osm} of the network

$$\Pi_{osm} + \Pi_{el} = 0 \quad (5)$$

Scaling theory predicts[34] and many experimental findings[35,36] indicate that

$$\Pi_{osm} = Bk_BT\varphi^{3\nu/(3\nu-1)} \quad (6)$$

where the constant B depends on the thermodynamic quality of the solvent. Fromg eqs 4−6, it follows that $A = B$.

The concentration dependence of the elastic pressure can be given as

$$\Pi_{el} = -G = -Ak_BT{\varphi_e}^{3\nu/(3\nu-1)-1/3}\varphi^{1/3} \quad (7)$$

where G is the shear modulus of the gel.

Thus, in the general case, when the gel is not in excess solvent, the osmotic swelling pressure ω is obtained from eqs 5−7

$$\omega = \Pi_{osm} - G = Ak_BT(\varphi^{3\nu/(3\nu-1)} - {\varphi_e}^{3\nu/(3\nu-1)-1/3}\varphi^{1/3}) \quad (8)$$

3. Experimental Section

3.1. Sample Preparation. Poly(vinyl alcohol) (PVA, M_n = 70 000−100 000, degree of hydrolysis >99 mol %) gel cylinders (1 cm diameter, 1 cm height) were cast with initial polymer concentrations of 3, 6, 9 and 12% (w/w) for osmotic swelling and macroscopic compression tests. Gel slabs (>2 mm thick) with initial polymer concentration of 6% (w/w) were cast for AFM nanoindentation. The gels were cross-linked with glutaraldehyde (one unit per 100 monomer units) at pH ≈ 1.5.[37] After gelation the gel slabs were washed in pure water to remove sol fraction, and then equilibrated with water/*n*-propyl alcohol mixtures containing gradually increasing amount of *n*-propyl alcohol. Swelling and mechanical tests were performed on the gels after 2−3 days.

3.2. Elastic (Shear) Modulus Measurements. Shear modulus data were obtained from uniaxial compression measurements using a TA.XT2I HR Texture Analyzer (Stable Micro Systems, UK). This apparatus measures the deformation (±0.001 mm) as a function of an applied force (±0.01 N). Stress−strain isotherms were determined for all gels in the fully swollen state and at different swelling ratios in pure water and in water/*n*-propyl alcohol mixtures. The PVA/water gels were equilibrated with poly(vinylpyrrolidone) solutions of known osmotic pressure according to a method described previously.[36−38] Gel samples were uniaxially compressed (at constant volume) between two parallel flat plates. The data were analyzed using the Mooney−Rivlin relation[27,39]

$$\sigma = C_1(\Lambda - \Lambda^{-2}) + C_2(\Lambda - \Lambda^{-2})\Lambda^{-1} \quad (9)$$

where σ is the nominal stress (related to the undeformed cross section of the gel), Λ is the deformation ratio ($\Lambda = L/L_0$, L and L_0 are the lengths of the deformed and undeformed specimen, respectively), and C_1 and C_2 are constants. Equation 9 is generally valid for extension measurements made on rubber-like materials. The stress−strain data were determined in the range of deformation ratio $0.7 < \Lambda < 1.0$. The value of C_2 was negligibly small for the gel systems studied. In this situation, the constant C_1 can be identified with the shear modulus (G) of the swollen network.

All swelling and mechanical measurements were made at 25 °C.

3.3. AFM Nanoindentation. Gel slabs were kept immersed in solution throughout the duration of the AFM measurements. General-purpose, oxide-sharpened, silicon nitride tips of pyramidal shape were used for the AFM measurements, performed using a commercial AFM (Bioscope SZ with Nanoscope V controller, Veeco). The spring constants of the cantilevers were measured by the thermal tune method. A raster scanning approach ("force−volume") was applied to automatically perform indentations over areas ranging from 10 μm × 10 μm to 30 μm × 30 μm at a resolution of 32 × 32 (1024 total indentations). Code written in Matlab was used to automatically process each data set and extract values of shear modulus using an optimization-based approach.[40] The shear modulus was extracted from each force-indentation curve using the relationship between force (F) and indentation depth (δ) for a pyramidal indenter derived by Bilodeau:[41]

$$F = \frac{1.4906G\tan\theta}{1-\mu}\delta^2 \quad (10)$$

where 2θ is the tip angle and μ is Poisson's ratio of the indented material.

Accuracy of elasticity measurements using the AFM is dependent upon methodology and modeling of the acquired force−deflection data.[40] Tapered tips are generally better suited

(35) Horkay, F.; Hecht, A. M.; Geissler, E. *J. Chem. Phys.* **1989**, *91*, 2706–2711.
(36) Horkay, F.; Zrinyi, M. *Macromolecules* **1982**, *15*, 1306–1310.
(37) Horkay, F.; Burchard, W.; Geissler, E.; Hecht, A. M. *Macromolecules* **1993**, *26*, 1296–1303.
(38) Vink, H. *Eur. Polym. J.* **1971**, *7*, 1411–1419.
(39) Treloar, L. R. G. *The Physics of Rubber Elasticity*, 3rd ed.; Oxford University Press: Oxford, 1975.
(40) Lin, D. C.; Dimitriadis, E. K.; Horkay, F. *J. Biomech. Eng.* **2007**, *129*, 430–440.
(41) Bilodeau, G. *J. Appl. Mech.* **1992**, *59*, 519–523.

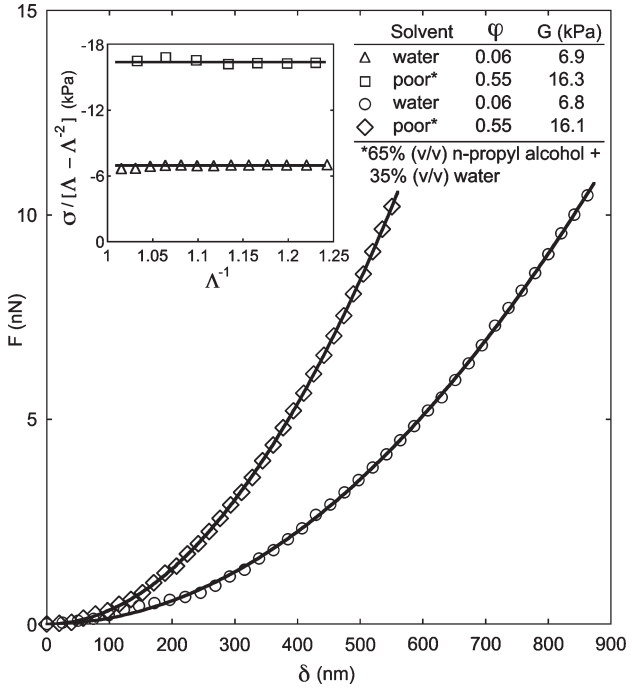

Figure 1. Sample AFM force (F)−indentation (δ) curves for PVA gels in water and the poor solvent. Equation 10 provides excellent fits in both cases (solid curves), indicating that the gels deformed linear elastically. Inset shows data from the macroscopic compression of PVA gel cylinders, also in water and the poor solvent. Equation 9 was used to fit the data; fits are represented by the solid lines.

for indenting materials with a large linear elastic limit.[40,42] They were selected over spherical probes in this study because of the greater resolution afforded. A tip velocity of ~800 nm/s was applied in all AFM indentation tests. We have shown previously[21,40] that this rate produces elastic behavior comparable to macroscopic compression of PVA gels. Standard techniques of mechanical property measurement such as macroscopic compression are appropriate means of calibration or validation of AFM measurements. In Figure 1, representative data sets from the AFM indentation of two PVA gels (one swollen in water and the other in 65% (v/v) *n*-propyl alcohol + 35% (v/v) water) are compared to corresponding macroscopic compression data to demonstrate the validity of our approach. The results show that the shear moduli obtained by the two independent techniques are in reasonable agreement.

Previous indentation experiments on PVA gels using spherical indenters had indicated that the linear elastic limit exceeded average strains of 5%.[21] Although tapered indenters induce greater strains,[42] it was found that at the maximum cantilever deflection of 100 nm applied in this study the force−indentation behavior still conformed to linear elastic equation (10), as shown in Figure 1. Additionally, an indenter with a tip diameter of several nanometers as is typical of probes used in this study can be considered sharp without introducing unacceptably large errors. Finally, the AFM data showed tip−sample adhesion to be negligible in the loading phase of the indentation, as is generally observed in soft samples.[43−48] This obviated the need to account for adhesive effects.

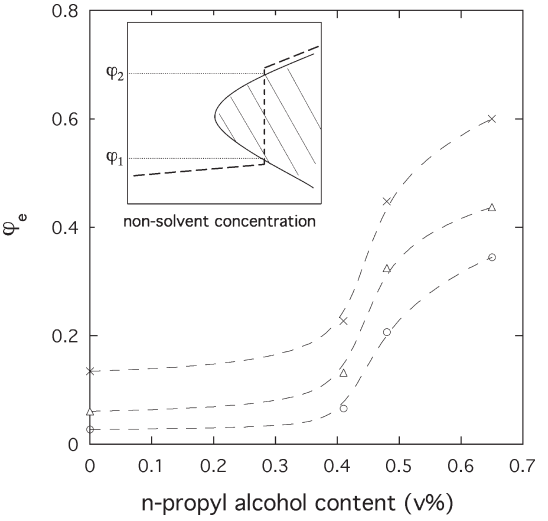

Figure 2. Swelling curves for PVA gels swollen in water/*n*-propyl alcohol mixtures. Polymer concentration at cross-linking: ○, 3% (w/w); Δ, 6% (w/w); ×, 12% (w/w). Inset: schematic phase diagram of a polymer gel. Hatched region is unstable.

4. Results and Discussion

4.1. Macroscopic Swelling and Mechanical Measurements. As discussed in the Theoretical Section, a characteristic feature of cross-linked polymers is their swelling ability; i.e., they can absorb (or expel) liquid due to changes in external conditions. In Figure 2 are shown typical swelling curves for PVA gels. These curves represent the volume fraction of the polymer in equilibrium with excess solvent (water/*n*-propyl alcohol mixture). On increasing *n*-propyl alcohol content, the polymer volume fraction increases. On the macroscopic scale probed in this experiment the volume transition appears continuous.

When a gel is in equilibrium with the surrounding solvent, its osmotic swelling pressure vanishes ($\omega = 0$). The region above the swelling curve corresponds to states with $\omega > 0$, while in region below the curve $\omega < 0$. On changing the solvent composition, the gel swells or shrinks until the new equilibrium state is attained. The inset illustrates schematically the phase diagram of a polymer gel. It appears similar to the miscibility curves usually observed for polymer solutions. In the hatched region the system is unstable. The solid line, often called the coexistence curve, represents the equilibrium condition. Systems inside this curve separate into two phases of compositions φ_1 and φ_2. The shape of the experimental swelling curves (dashed lines in Figure 2) is reminiscent of the phase diagram of gels.

As illustrated in Figure 2, the swelling degree ($1/\varphi_e$) decreases with increasing *n*-propyl alcohol concentration. Figure 3 shows the variation of the equilibrium shear modulus measured for PVA gels in different water/*n*-propyl alcohol mixtures. In each solvent mixture, the shear modulus G_e can be related to the polymer concentration φ_e by the scaling relation of the form $G_e = Ak_BT\varphi_e^{\nu}$. The prefactor Ak_BT varies from 3400 kPa (in pure water) to 4100 kPa [in 65% (v/v) *n*-propyl alcohol + 35% (v/v) water mixture]. The inset shows the variation of n and ν with the solvent composition. In pure water n (≈2.3) is close to the theoretical value in good solvent condition and gradually increases with decreasing solvent quality. The excluded volume

(42) Dimitriadis, E. K.; Horkay, F.; Maresca, J.; Kachar, B.; Chadwick, R. S. *Biophys. J.* **2002**, *82*, 2798–2810.
(43) Butt, H.; Capella, B.; Kappl, M. *Surf. Sci. Rep.* **2005**, *59*, 1–152.
(44) Jacot, J. G.; Dianis, S.; Schnall, J.; Wong, J. Y. *J. Biomed. Mater. Res. A* **2006**, *79*, 485–494.
(45) Jandt, K. D. *Surf. Sci.* **2001**, *491*, 303–332.
(46) Lin, D. C.; Horkay, F. *Soft Matter* **2008**, *4*, 669–682.
(47) Sun, Y.; Akhremitchev, B.; Walker, G. C. *Langmuir* **2004**, *20*, 5837–5845.
(48) Tsukruk, V. V.; Huang, Z.; Chizhik, S. A.; Gorbunov, V. V. *J. Mater. Sci.* **1998**, *33*, 4905–4909.

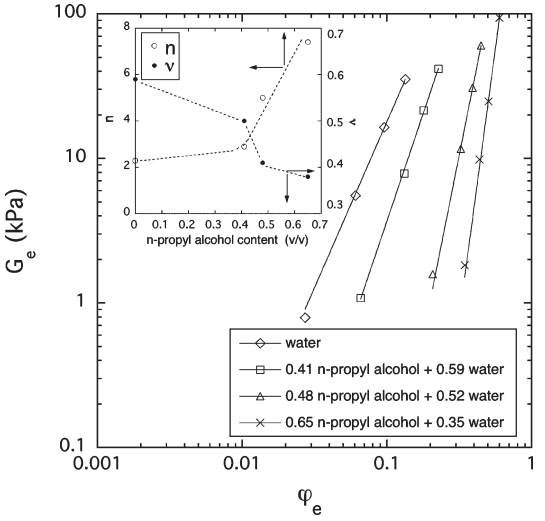

Figure 3. Shear modulus as a function of polymer volume fraction φ_e in four solvents of varying quality. Continuous curves are least-squares fits to $G_e = Ak_BT\varphi_e{}^n$. Inset shows the variation of n and ν (excluded volume exponent) as a function of the n-propyl alcohol content of the equilibrium solvent mixture.

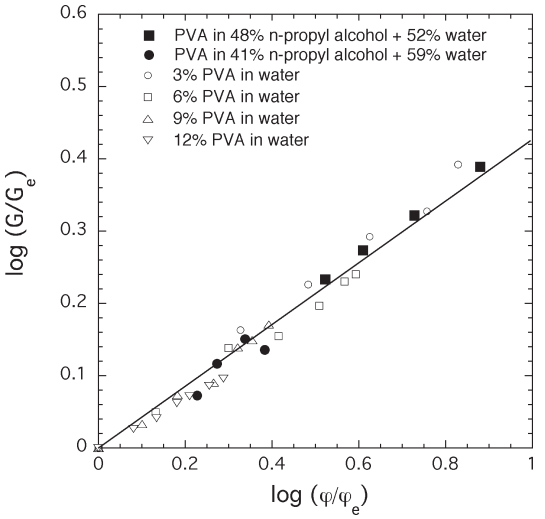

Figure 4. Log−log plot of normalized shear modulus (G/G_e, where G_e is the shear modulus in equilibrium with pure water) as a function of normalized polymer concentration (φ/φ_e, where φ_e is the polymer volume fraction of the fully swollen gel in water) for PVA gels in water (open symbols) and in water/n-propyl alcohol mixtures (filled symbols). The slope of the straight line through the data points is 0.42.

exponent ν decreases with increasing n-propyl alcohol content and approaches the value corresponding to collapsed polymer chains ($\nu \rightarrow 1/3$).

Addition of a nonsolvent decreases the thermodynamic quality of the solvent and thus reduces the swelling capacity of the network. However, changes in the thermodynamic interactions may also affect the structure and the elastic properties of the gel. To determine the effect of the composition of the solvent/nonsolvent mixture on the shear modulus of PVA gels, we plotted G/G_e as a function of φ/φ_e (Figure 4), where G and φ are the shear modulus and the polymer volume fraction in the mixed solvent, respectively, and G_e and φ_e are the corresponding quantities in water. In the figure are also displayed the values of G/G_e determined in water at different PVA concentrations (open sysmbols). It is clear from this double logarithmic representation

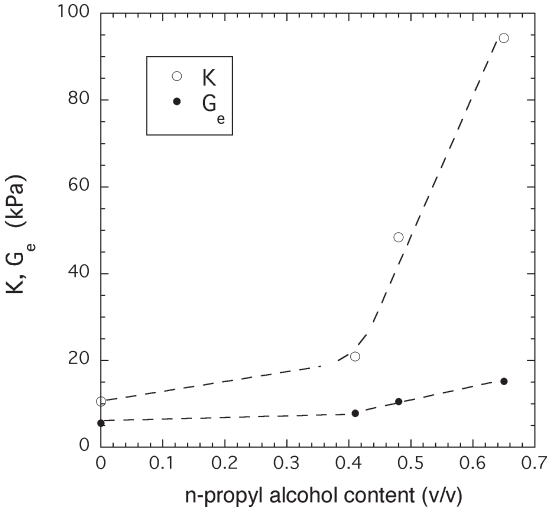

Figure 5. Variation of K and G_e for a PVA gel (cross-linked at 6% (w/w) polymer concentration) as a function of the n-propyl alcohol concentration in n-propyl alcohol/water mixtures.

that all data fit the power law relationship

$$G/G_e = (\varphi/\varphi_e)^n \tag{11}$$

where the exponent ($m \approx 0.42$) slightly exceeds the value 1/3 predicted by the theory of rubber elasticity.[39] The observed universal behavior implies that the elastic modulus is primarily determined by the overall polymer concentration; i.e., changes in the polymer−solvent interactions do not affect the number of elastic chains. This finding is consistent with previous results obtained for various polymer gels in different solvent conditions.[35,49]

As we have seen, changes in the solvent quality affect the osmotic swelling pressure and thus the equilibrium concentration of polymer gels. The osmotic modulus K [$= \varphi(\partial\omega/\partial\varphi)$] defines the resistance of the gel to changes in the swelling degree. As shown above (see eq 8), ω contains two contributions: (i) the osmotic pressure of the network chains that is the driving force of the swelling process and (ii) the shear modulus that counteracts the osmotic pressure and preserves the shape of the gel. It follows from eq 8 that the osmotic modulus is given by

$$K = Ak_BT(n\varphi^n - m\varphi_e{}^{n-m}\varphi^m) \tag{12}$$

Figure 5 shows the variation of K and G for PVA gels in different n-propyl alcohol/water mixtures. It can be seen that K sharply increases with decreasing solvent quality in the transition region while the variation of G is much less pronounced.

4.2. Construction of Elastic and Osmotic Modulus Maps. So far we have discussed the effect of solvent composition on the macroscopic swelling and elastic behavior of PVA gels. We have seen that both the polymer concentration and the shear modulus increase continuously through the transition. This result is consistent with the picture that in the phase separating gel the nuclei of the new phase are randomly formed and distributed in space and the two phases coexist locally over the entire sample. In what follows we investigate the spatial variation of the shear and osmotic moduli by combining AFM measurements with macroscopic swelling pressure observations. To gain insight into the effect of changes in the structure and interactions occurring

(49) Horkay, F.; McKenna, G. B. In *Physical Properties of Polymers Handbook*, 2nd ed.; Mark, J. E., Ed.; Springer: New York, 2007; pp 497−524.

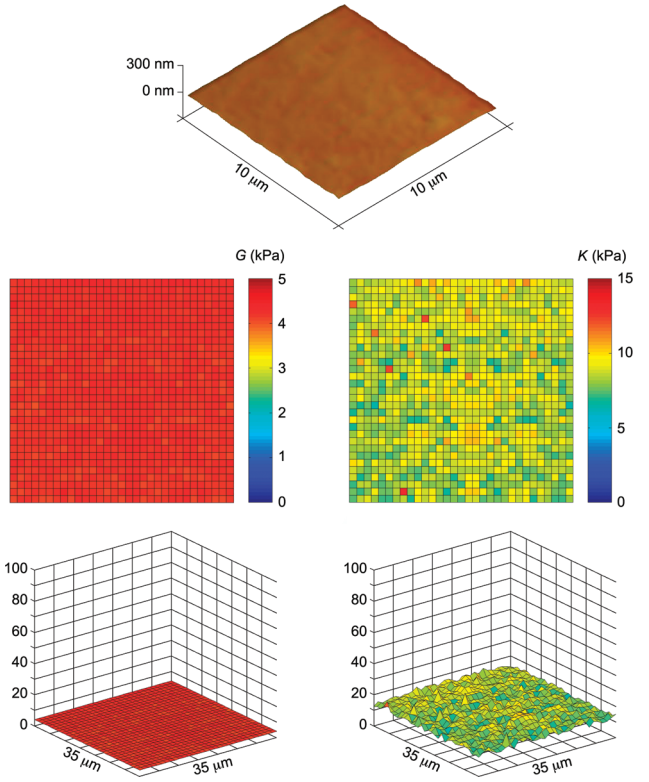

Figure 6. AFM topography image (top), 2D and 3D shear modulus maps (left), and 2D and 3D osmotic modulus maps (right) of a PVA gel [cross-linked at 6% (w/w) polymer concentration] in pure water.

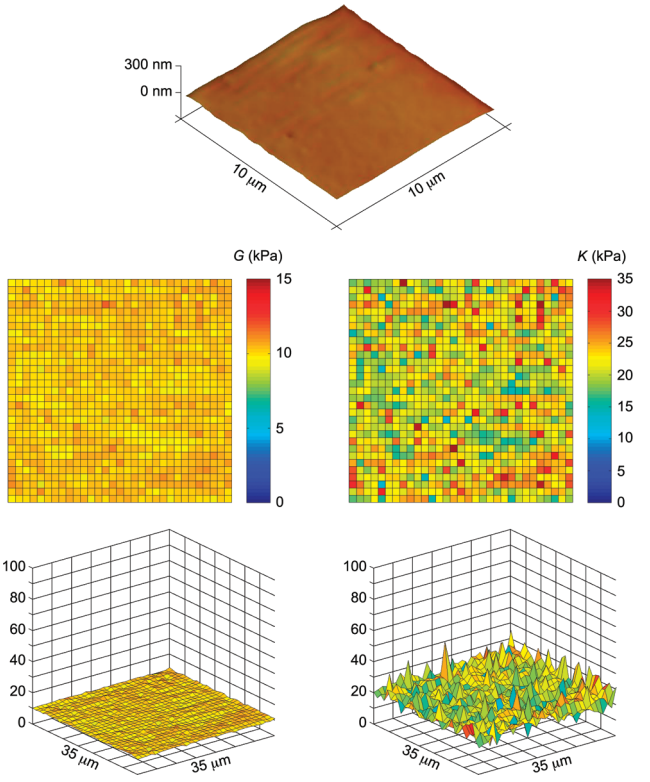

Figure 7. AFM topography image (top), 2D and 3D shear modulus maps (left), and 2D and 3D osmotic modulus maps (right) of a PVA gel in a solution of 41% (v/v) *n*-propyl alcohol + 59% (v/v) water, close to the theta condition. The gel sample is the same as in Figure 6.

at high resolution, we construct the elastic and osmotic modulus maps of the PVA gels at different stages of phase separation.

In the region below the spinodal decomposition little is known about the structure and dynamics of polymer gels. The transport of solvent molecules between the gel and the surrounding liquid phase is a diffusion-controlled process, during which concentration inhomogeneities gradually develop. De Gennes discussed theoretically the phase behavior of polymer gels.[34] Onuki[50] constructed a model for gels undergoing spinodal decomposition and showed that in the late stage the growth rate slowed down due to the elastic forces imposed by the network. It has been found that on the mesoscopic level the gel is composed of highly concentrated collapsed domains separated by lower concentration swollen regions. These domains can slowly coalesce and segregate. Domain formation strongly affects the local physical properties (e.g., elastic modulus) of the system.

Shear and osmotic modulus maps for PVA gels in different *n*-propyl-alcohol/water mixtures are shown in Figures 6 to 8, where the 3D plots have been scaled identically to facilitate comparison between the different cases. The shear modulus maps were directly obtained from the AFM force−indentation measurements. The elasticity−concentration relationships displayed in Figures 3 and 4 are representative of the prerequisite data for generating maps of K: for each point on the shear modulus map the local polymer concentration in the gel was estimated from the measured value of the local shear modulus assuming that the macroscopic scaling relationship applies on the microscopic level.

Figure 6 shows that in water the surface of the PVA gel is smooth, and both G_e and K exhibit only small local variations ($4 < G_e < 5$ kPa and $5 < K < 15$ kPa) at the micrometer length scale.[14] As the solvent quality decreases, nonuniformities in polymer concentration arise throughout the gel; K, and to a much lesser extent, G, reflect these inhomogeneities. This trend is clearly visible in comparing the AFM topographaphical images and shear modulus maps in Figures 6−8. In the case of the Θ-solvent (Figure 7), surface topography and local shear moduli remain relatively uniform. However, the increased amplitude of K is an indication of the onset of phase separation.

In gels inhomogeneous structures develop during volume phase transition. The size and shape of the polymer-rich domains as well as the volume ratio between the swollen and shrunken regions of the sample are a function of the solvent composition. The structural changes induced by the transfer of solvent molecules from the surrounding liquid phase into the network first take place at the gel surface and then gradually extend into the bulk. However, the gel surface attains equilibrium only after the bulk. The present results show that surface and bulk patterns strongly affect the local elastic and osmotic response of the PVA gels. This becomes evident in the poor solvent (Figure 8) where even the surface topography and the shear modulus exhibit significant spatial variations. The map of K contains peaks and valleys, demonstrating the strong dependence of the local value of K on polymer concentration distribution. The shear and the osmotic moduli vary in the range $5 < G_e < 20$ kPa and $10 < K < 90$ kPa, respectively.

4.3. Significance and Outlook. The importance of gaining better physical understanding of the phase behavior of gels is obvious if we note the occurrence of gel-like materials in nature, particularly in living systems. The structure and properties of many composite materials are controlled by their phase

(50) Onuki, A.; Puri, S. *Phys. Rev. E* **1999**, *59*, R1331–R1334.

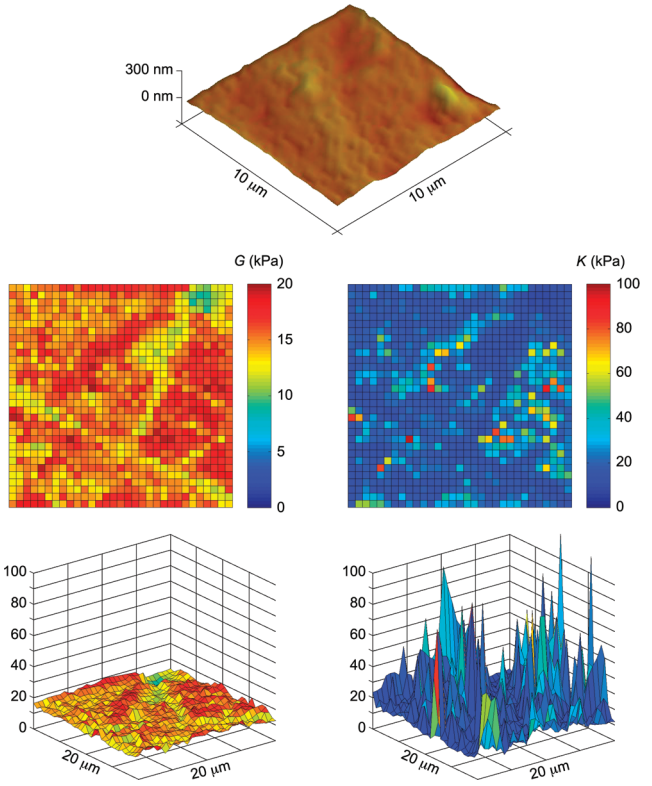

Figure 8. AFM topography image (top), 2D and 3D shear modulus maps (left), and 2D and 3D osmotic modulus maps (right) of a PVA gel in a solution of 65% (v/v) *n*-propyl alcohol + 35% (v/v) water (poor solvent condition). The gel sample is the same as in Figures 6 and 7.

behavior. In chemically cross-linked polymer gels various patterns of volume phase transition have been observed. The osmotic modulus map provides a detailed, high-resolution picture of swelling and elastic properties of gels along with a quantitative assessment of local inhomogeneity.

AFM nanoindentation is a widely applied technique for mapping the elasticity of inhomogeneous samples, such as biological cells and tissues, at high resolution.[8,10,11,14,20,51−55] One of the chief advantages of this method is its capability to simultaneously measure the topography of the scanned region. To the best of our knowledge, the work presented herein represents the first time that the AFM has been used in tandem with osmotic swelling pressure measurements to map the osmotic modulus of gels, which is more reflective of local changes in composition and thermodynamic interactions than the elastic properties alone.

Swelling of polymer films is important in applications ranging from coatings and sensors to microelectronics and biomedical devices. Soft contact lenses represent an example where performance, comfort, and even eye health are influenced by local mechanical and hydration properties.[56] In this case, a means of mapping the elastic and osmotic moduli at high resolution is essential in assessing local inhomogeneities and improving performance.

The osmotic modulus map allows us to predict both elastic response and recovery capability of complex viscoelastic materials and is particularly important to estimate the compressive behavior of biological tissues. For instance, it is known that a decrease in the shear modulus of articular cartilage results in reduced compressive resistance and hence compromised load-bearing capacity.[57] A relatively smooth map of K (Figure 6) indicates that resorption of water occurs consistently throughout the sample while large disparities in K (Figure 8) signify nonuniform volumetric recovery. It can be deduced from Figure 8 that regions of slightly different shear modulus can exhibit drastic differences in recovery behavior. For example, in articular cartilage of the knee and hip, which can experience large-amplitude repetitive loading during physical activity (e.g., walking), rapid recovery of the bulk tissue is crucial to normal function. A decrease in the osmotic pressure at the tissue level is associated with degenerative conditions such as osteoarthritis.[4,5,25,58] We surmise that changes in microscopic osmotic properties are complicit as a pathological feature of osteoarthritis.

5. Conclusions

The osmotic modulus is a measure of the contribution of osmotic pressure and elastic modulus to the compressive resistance of polymer gels. By relating K and G through concentration-dependent scaling laws, we have demonstrated that K is significantly more sensitive to polymer concentration gradients than G. The two quantities are complementary, serving to describe the swelling and shape preservation tendencies of soft gel-like materials. The osmotic mapping technique proposed herein allows local variations in K to be determined by combining nano- and microindentation instrumentation with macroscopic osmotic swelling pressure observations. The osmotic modulus map provides insight into the effect of structural changes (e.g., self-assembly) on the swelling and elastic properties of gel systems at high resolution. This knowledge is essential in biomechanical studies, such as tissue characterization and the development of biomimetic tissue analogues, and may also help to assess the performance of gel-like materials used in biomedical devices.

Acknowledgment. This work was supported by the Intramural Research Program of the NIH, NICHD.

(51) A-Hassan, E.; Heinz, W. F.; Antonik, M. D.; D'Costa, N. P.; Nageswaran, S.; Schoenenberger, C.; Hoh, J. H. *Biophys. J.* **1998**, *74*, 1564–1578.
(52) Almqvist, N.; Bhatia, R.; Primbs, G.; Desai, N.; Banerjee, S.; Lal, R. *Biophys. J.* **2004**, *86*, 1753–1762.
(53) Haga, H.; Sasaki, S.; Kawabata, K.; Ito, E.; Ushiki, T.; Sambongi, T. *Ultramicroscopy* **2000**, *82*, 253–258.
(54) Stolz, M.; Raiteri, R.; Daniels, A. U.; VanLandingham, M. R.; Baschong, W.; Aebi, U. *Biophys. J.* **2004**, *86*, 3269–3283.
(55) Touhami, A.; Nysten, B.; Dufrene, Y. F. *Langmuir* **2003**, *19*, 4539–4543.
(56) Opdahl, A.; Kim, S. H.; Koffas, T. S.; Marmo, C.; Somorjai, G. A. *J. Biomed. Mater. Res. A* **2003**, *67*, 350–356.
(57) Roberts, S.; Weightman, B.; Urban, J.; Chappell, D. *J. Bone Jt. Surg., Br. Vol.* **1986**, *68*, 278–288.
(58) Basser, P. J.; Schneiderman, R.; Bank, R. A.; Wachtel, E.; Maroudas, A. *Arch. Biochem. Biophys.* **1998**, *351*, 207–219.